Journal of Magnetic Resonance 198 (2009) 151–159

Contents lists available at ScienceDirect

Journal of Magnetic Resonance

journal homepage: www.elsevier.com/locate/jmr

Design of self-refocused pulses under short relaxation times

Bashar Issa *

Department of Physics, College of Science, University of UAE, P.O. Box 17551, Al-Ain, AD, United Arab Emirates

ARTICLE INFO

Article history:
Received 29 September 2008
Revised 2 February 2009
Available online 10 February 2009

Keywords:
Selective excitation
Relaxation
Bloch equations
Simulated annealing
Radio frequency pulse

ABSTRACT

The effect of using self-refocused RF pulses of comparable duration to relaxation times is studied in detail using numerical simulation. Transverse magnetization decay caused by short T2 and longitudinal component distortion due to short T1 are consistent with other studies. In order to design new pulses to combat short T1 and T2 the relaxation terms are directly inserted into the Bloch equations. These equations are inverted by searching the RF solution space using simulated annealing global optimization technique. A new T2-decay efficient excitation pulse is created (SDETR: *s*ingle *d*elayed *e*xcursion *T2* *r*esistive) which is also energy efficient. Inversion pulses which improve the inverted magnetization profile and achieve better suppression of the remaining transverse magnetization are also created even when both T1 and T2 are short. This is achieved, however, on the expense of a more complex B1 shape of larger energy content.

1. Introduction

When imaging samples with very short T2 (e.g. bone, tissue injected with contrast agent, or porous media) it is desirable to start acquiring signal immediately after the end of the RF excitation pulse. This has been achieved using self-refocused pulses which remove the need for applying gradient reversal usually needed for rewinding spins' accumulated linear phase. The family BURP (*b*and-selective *u*niform-*r*esponse *p*ure-phase) RF pulses [1] have been designed using optimization techniques. Although these pulses shorten total excitation time spins still relax during the excitation leading to reduced NMR signal. In many cases the design criteria have ignored relaxation processes by assuming that both relaxation times T1 and T2 are much longer than the RF pulse duration (L). While this assumption is correct in many cases especially when short RF pulses (known as hard pulses) are used to excite bulk samples, however, there are applications in which relaxation times have to be taken into account when they become comparable to L. For example T1 is shortened considerably in T1-weighted dynamic contrast-enhanced imaging and also when paramagnetic impurities and surface relaxation make T1 comparable to L in porous media imaging.

Many studies have analyzed the effect of short relaxation times (in particular T2) on the NMR signal [2–6]. This was done by inserting already known RF profiles (e.g. Burp, Gaussian, sinc, SNOB, etc.) into the *forward* calculation of the Bloch equations using numerical techniques. Others have attempted to take into account the effects of relaxation into the design of the RF pulse [3,7–9]. This is usually a more demanding problem since it involves *inverting* the Bloch equations and the design will be tailored to specific value of T1 and T2, and therefore may not be optimum for exciting all values of T1 and T2.

Results obtained here confirm most of the studies referenced in this work that short T2 attenuate magnetization in the selected slice region while short T1 produce significant distortions in the profiles. We extend this work by seeking new slice-refocused RF profiles that reduce the effects of short relaxation times.

2. Theory

We use simulated annealing (SA) global optimization techniques [1,10–12] to synthesize self-refocused RF pulses (B1 profiles). Typically the annealing procedure relies on gradually reducing an initial value (T_0) of a control parameter (temperature analog in thermodynamics) by a small amount (temperature step ΔT). At each temperature a series (N) of random search processes are performed to search for the minimum of an error function at certain system configuration. The system variables are the set of desired B1 values. The error is the mean square difference between the target response and the excited magnetization. The latter is calculated by numerically solving the Bloch equations, using Runge–Kutta–Fehlberg 6th order method [13]. In this work, and unlike previously published reports on SA, we include the relaxation terms in the Bloch equations to investigate the RF profiles under conditions when T1 and T2 are comparable to L. The Bloch equations then become as in Eq. (1)

$$\frac{\partial \vec{M}}{\partial t} = \gamma(\vec{M} \times \vec{B}) - R\vec{M} + R1\vec{M}_0 \tag{1}$$

where $\vec{M} = (M_x, M_y, M_z)^T$ is the magnetization column vector, $\vec{B}$ is the effective RF field in the laboratory frame, and γ is the gyromag-

* Fax: +971 3 7671 291.
E-mail address: b.issa@uaeu.ac.ae

1090-7807/$ - see front matter © 2009 Elsevier Inc. All rights reserved.
doi:10.1016/j.jmr.2009.02.001

netic ratio. R is a 3×3 diagonal matrix with elements $R2$, $R2$, and $R1$, and $\vec{M}_0 = (0, 0, M_0)^T$ is the thermal equilibrium magnetization column vector.

The frequency response is discretized into M elements covering the slice selection direction for the three magnetization components (M_{ij}, $i = 1, 2, 3$ for the x, y, and z components respectively, and $j = 1$ to M for the space elements). The target magnetization profile (M_{ij}^{target}, with similar meaning for the indices i and j as before) is the desired magnetization response due to the application of the RF pulse. The RF pulse can be, for example, a $\pi/2$ excitation pulse or a π inversion pulse. The objective (or error) function (Eq. (2)) that we seek to minimize is

$$objective = \sum_{i=1}^{3} \sum_{j=1}^{M} \left(M_{ij}^{\text{target}} - M_{ij} \right)^2 \tag{2}$$

Constraints on the maximum and minimum permissible values of the magnetization components (M_{ij}^{upper} and M_{ij}^{lower}) are also defined. The number of the constraints along each axis can be smaller than the maximum M if some regions of the frequency response are left unconstrained for some or all of the magnetization components. For example, the transition region between the excited slice and suppression (unexcited) regions is unconstrained for all magnetization components, while the M_z component is left free in the excited slice region for the excitation pulse [1]. For this work we have constrained all magnetization components according to Eq. (3) to design a $\pi/2$ excitation pulse

$$\left.\begin{array}{ll} -\varepsilon_{lower} < M_x < \varepsilon_{upper}; & \text{for all } v \\ M_0 - \varepsilon_{lower} < M_y < M_0 & \text{for } |v| < \Delta F/2 \\ -\varepsilon_{lower} < M_y < \varepsilon_{upper}; & \text{for } |v| > \Delta F/2 + \delta F \\ -\varepsilon_{lower} < M_z < \varepsilon_{upper}; & \text{for } |v| < \Delta F/2 \\ M_0 - \varepsilon_{lower} < M_z < M_0; & \text{for } |v| > \Delta F/2 + \delta F \end{array}\right\} \tag{3}$$

M_0 is set to unity and $\varepsilon_{\text{lower}}$ and $\varepsilon_{\text{upper}}$ are the tolerance values (set to 0.001). ΔF is the slice thickness and δF is the transition region width, both in Hz.

In order to speed up the optimization process the constrained problem is transformed into an unconstrained one. This is achieved by inserting the constraints into the error function using the method of penalties [13,14]. The contribution of the constraints is controlled through the weighting or emphasis factors α_i, $i = 1, 2, 3$ for the x, y, and z components, respectively (chosen for the results presented here to be equal to each other). The objective function then becomes

$$objective = \sum_{i=1}^{3} \left\{ \sum_{j=1}^{M} \left(M_{ij}^{\text{target}} - M_{ij} \right)^2 + \alpha_i \left(\sum_{j=1}^{M} \left(M_{ij}^{upper} - M_{ij} \right)^2 + \sum_{j=1}^{M} \left(M_{ij}^{lower} - M_{ij} \right)^2 \right) \right\} \tag{4}$$

L is chosen to be 3.0 ms and modeled discretely by 30 ordinates and the maximum number of constraints M is set to 64 in this work. Searching the error surface for the minimum error is accomplished by varying the B1 profile. This is implemented indirectly through the use of Fourier series coefficients [1,11] with six harmonics yielding a total of 13 adjustable coefficients. This procedure ensures continuous and smooth RF profile [15] and reduces the computational task by searching through a smaller dimensional space (i.e. 13 instead of 30). The B1 waveform is given by Eq. (5)

$$\text{B1}(t_i)P = a_0 + \sum_{n=1}^{6} a_n \cos(n w_0 t_i) + b_n \sin(n w_0 t_i) \qquad i = 1, 2, \ldots, 30 \tag{5}$$

$w_0 = 2\pi/L$ is the fundamental frequency.

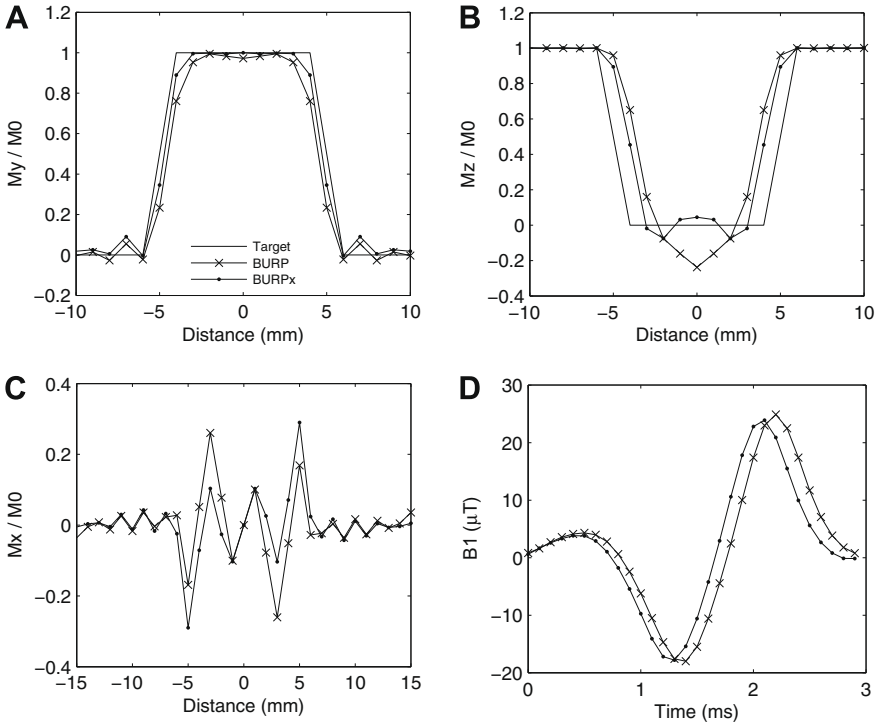

Fig. 1. A $\pi/2$ excitation pulse is optimized using constraints applied to all magnetization components over all frequency regions (extended constraints BURPx) as opposed to the BURP pulses (which have no constraints over the z-component). Excited magnetization component is improved slightly (A and B). Furthermore, the BURPx profile (D) appears slightly shorter than BURP and therefore will be adopted as a standard for comparison with other designed pulses in this work. Similar out of phase transverse magnetization (C) are produced by the two pulses.

We investigate the effect of different values of T1 and T2 on the design of the RF profile and hence the magnetization response. Combinations of T1 and T2 values include infinite T1 and T2 (values set to 1×10^{15} seconds in the programming code) along with three other values: $L/2$, L, and $2L$. The design of pulses will consider both excitation and inversion pulses. We also emphasize the importance of careful selection of the optimization parameters on the type of RF pulse produced by the simulation annealing process. Among these parameters are the weighting coefficients α_i (taken to be all equal to 0.1 in the results presented here), temperature step ($\Delta T \sim 0.005$ to 0.1), the maximum number of search iterations ($N \sim 3000$ to 10,000) at each temperature, and the initial temperature $T_0 \sim 2.0$.

3. Results

The effect of extending the range of the applied constraints to all regions of the frequency response for the three magnetization components is shown in Fig. 1. Both responses from the standard BURP [1] pulse and that of the extended-constraints pulse (referred to as BURPx) are overlaid with the target response for the transverse and longitudinal components. Both relaxation times are assumed infinite compared to pulse duration (T1 and T2 $\sim$ inf). The response profiles are very similar to each other (as expected due to the similar constraints) with slight improvement in the slice delineation using the extended constraints method (Fig. 1A and B show BURPx magnetization closer to the target than those pro-

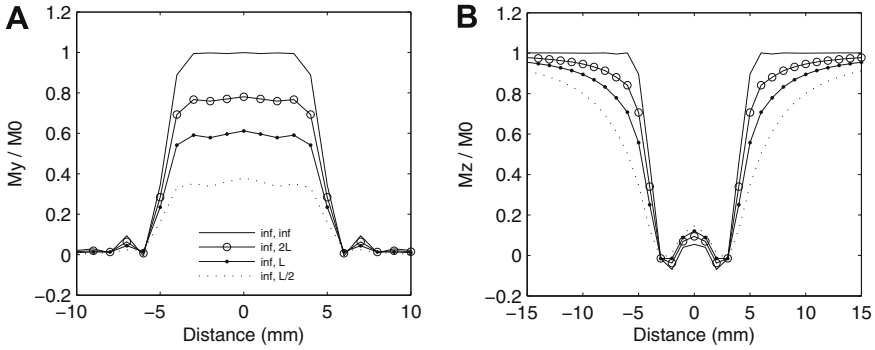

Fig. 2. The BURPx RF profile that was optimized for infinite relaxation times is tested for samples of shorter T2 (T1 $\sim$ inf). As expected the absorbed magnetization (M_y) suffers increasing decay with decreasing T2 (A) while the longitudinal component exhibits greater broadening (B). The dispersion transverse profile (not shown here) suffers similar decay as experienced by the absorption component. Values of T2 are inf, $2L$, L, and $L/2$ while T1 $\sim$ inf.

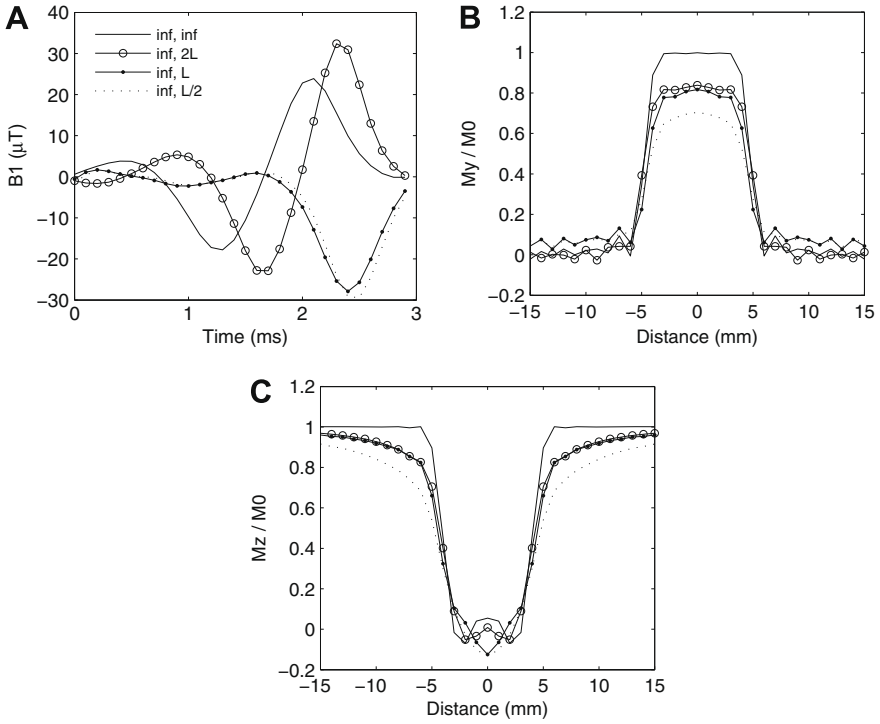

Fig. 3. A T2 attenuation resistant RF pulse (SDETR) is optimized. SDETR exhibits a single main delayed RF excursion which leaves magnetization vector closer to transverse plane for shorter time and hence less T2 decay. T2 values are directly inserted into the design (RF synthesis) process by including relaxation terms into Bloch equations. This yielded new RF profiles (A) according to the T2 value used. Initially when T2 is reduced to $2L$ the design responds by maintaining the same RF profile but increasing its amplitude. When T2 is reduced further a more efficient RF profile becomes necessary (SDETR). The transverse and longitudinal magnetization components produced by various RF profiles are shown in (B–C), respectively, and its amplitude reflects the corresponding T2 values.

duced by BURP). As expected the RF profiles have the same general shape and similar peak values except that the extended-constraints pulse peaks at a slightly earlier time and it appears shorter than BURP by 3%. Geen and Freeman [1] adopted similar approach by extending the range of the constraints for the dispersion component in order to improve phase purity. In all results to follow we have adopted the all constraints method (BURPx).

To show the effect of short T2 on the excited magnetization the $\pi/2$ BURPx pulse (that was optimized under infinite values of T1 and T2) will be tested with samples of small T2. BURPx is used in the forward calculation of Bloch equations, however, with three shorter T2 values: T2 = $L/2$, L, and $2L$ (Fig. 2). The absorption profile suffers a corresponding decreasing magnitude ~40%, 60%, and 75% of that corresponding to infinite T2, but little degradation in the shape of the profile (Fig. 2A). The longitudinal component suffers increasing broadening while the dispersion magnetization is diminishing with decreasing T2 (Fig. 2B–C). This behavior would be similar to other pulses such as BURP, Gaussian, sinc, etc. We attempt to reduce this transverse magnetization decay.

Thus far we have concerned ourselves with the design of a refocused pulse under ideal relaxation conditions, i.e. infinite T1 and T2. We turn our attention now to the *design* of RF pulses under short T2 (T1 is kept infinite initially). The relaxation decay terms are included into the Bloch equations used to search the solution space for RF pulses with short values for T1 and T2. Different optimized RF profiles are shown in Fig. 3A. Decreasing T2 from infinity to T2 = $2L$, yielded a similar RF pulse to BURPx with delayed peaks, and larger amplitude of the maximum peak (36%). However, decreasing T2 further (i.e. T2 = L and $L/2$) yielded a new RF profile that has a single main peak delayed to the end of the RF duration. We refer to this pulse SDETR: *s*ingle *d*elayed *e*xcursion *T2* *r*esistive pulse. The magnetization produced by these four pulses is shown in Fig. 3B–C and its amplitude reflects the values of T2.

The improved performance of the new SDETR pulse is detailed in Fig. 4 which shows a comparison between SDETR and BURPx pulses and is emphasized by an additional comparison with a standard non-refocused sinc pulse. The relative gain in the absorption magnetization produced by SDETR pulse is larger for smaller T2

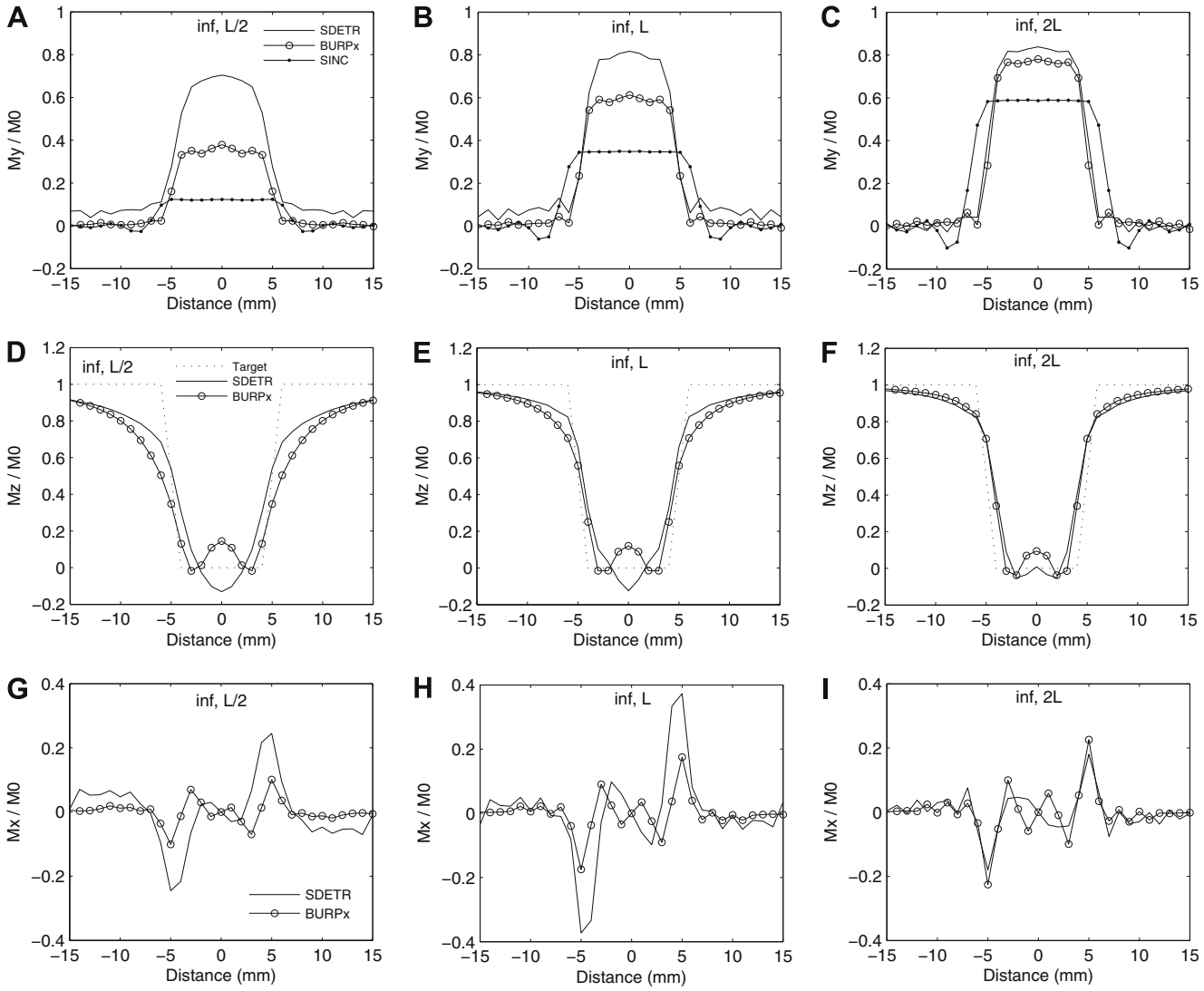

Fig. 4. The transverse magnetization gain produced using SDETR (optimized for short T2) is emphasized in comparison with BURPx (optimized for infinite T2) and a standard non-refocused sinc pulses over different T2 values. M_y values for SDTER and BURPx pulses are: $0.7M_0$ and $0.4M_0$ at T2 = $L/2$, $0.8M_0$ and $0.6M_0$ at T2 = L, and $0.85M_0$ and $0.75M_0$ at T2 = $2L$. The gain in the absorption profile is sometimes offset by a larger undesired dispersion component (G–I) while the M_z components are similar (D–F). The title of the figure represents the values of T1 and T2 used in the calculation of the magnetization (i.e. forward calculation of the Bloch equations) while the legend shown inside the figure indicates the values used in the synthesis of the RF pulses.

values as clearly shown in Fig. 4A–C. The excited magnetization reaches magnitudes of 70%, 80%, and 85% of that corresponding to infinite T2 (i.e. compared to those produced by BURPx) for the T2 values of L,/2, L, and 2L respectively. Recall that applying BURPx under short T2 values produces 40%, 60%, and 75% magnetization peaks only (Fig. 2A and 4A–C). The longitudinal and dispersion transverse components are shown in Fig. 4D–F and G–I, respectively. The dispersion profiles produced by SDETR are of higher amplitude than BURPx. Notice comparison with BURPx is almost equivalent to comparison with the standard Geen pulse BURP due to similar profiles and magnetization.

We extend the RF synthesis by studying T1 relaxation next. RF excitation pulses have been optimized under short T1 and T2 conditions and the resulting profiles are compared with those produced by BURPx (i.e. infinite T1 and T2). Three sets of values are chosen for T1 and T2: L/2, L, and 2L (satisfying the obvious limit of T2 $\leqslant$ T1). Generally the RF profiles depart from the standard BURPx shape with more than one single RF excursion of dominant amplitude, and generally larger amplitude for the peaks (Fig. 5A). The absorption response and the longitudinal profiles are shown in Fig. 5B–C for the four pulses shown in Fig. 5A. We now compare these T1 and T2 optimized pulses (abbreviated as T12 pulses) with BURPx and standard sinc pulses. Although larger absorption profile is produced with the T12 pulses than BURPx (for T1 = T2 = L/2 and L but not for 2L), however, significant distortion exists in both pulses (Fig. 6A–C). This characteristic "melting" down effect has been reported before by Hajduk et al. [5] and Nullizard and Freeman [7] where shoulders droop down relative to the center. The dispersion profiles (Fig. 6G–I) show similar amplitudes, however, with more oscillations for the T12 optimized pulses than for BURPx.

Fig. 7A shows a π inversion pulse optimized under infinite T1 and T2 values (I-BURPx) along with the magnetization response (Fig. 7B). This is basically the pulse produced by Geen and Freeman [1]. The objective is to produce a fully inverted longitudinal component within the selected slice in addition to minimal transverse magnetization. Although dephasing gradient lobes can be applied after slice selection to nullify the remaining transverse magnetization (Fig. 7B) this would be considered undesirable for applications with short T2. The objective of the following optimization is to reduce remaining transverse magnetization while improving or at least not compromising M_z. Pulses are optimized for various combinations of T1 and T2 and the excited magnetization will be compared with those produced by standard I-BURPx pulse (optimized under infinite values of T1 and T2—Fig. 7A). The results can be summarized as follows:

- T1, T2 = (inf, L/2), Fig. 8A–D: the optimized pulse has smaller both peak amplitude and energy. It also exhibits a single large excursion similar to SDETR, however, followed and preceded by smaller excursions. While the inverted magnetization is very similar to that produced by I-BURPx the transverse components are greatly reduced (Fig. 8C–D) which represents great advantage.
- T1, T2 = (inf, L), results not shown here: similar pulse profile and magnetization response to those for (T1, T2) = (inf, L/2) above.
- T1, T2 = (L/2, L/2), Fig. 8E–H: imposing short T1 in addition to short T2 in the optimization procedure produces a multi-peak RF pulse with larger power and energy. The inverted magnetization (Fig. 8F) is much cleaner than that produced by a pulse which did not take into account the sample's short T1 and T2.
- T1, T2 = (L, L), results not shown here: the optimized pulse improves M_z while the transverse components produced are similar to the case discussed above.

We have demonstrated that simultaneously T1 and T2 optimized inversion pulses offer improved longitudinal and transverse magnetization responses.

In order to emphasize the stability of these new designed pulses we have applied the SDETR pulse (π/2 excitation optimized under

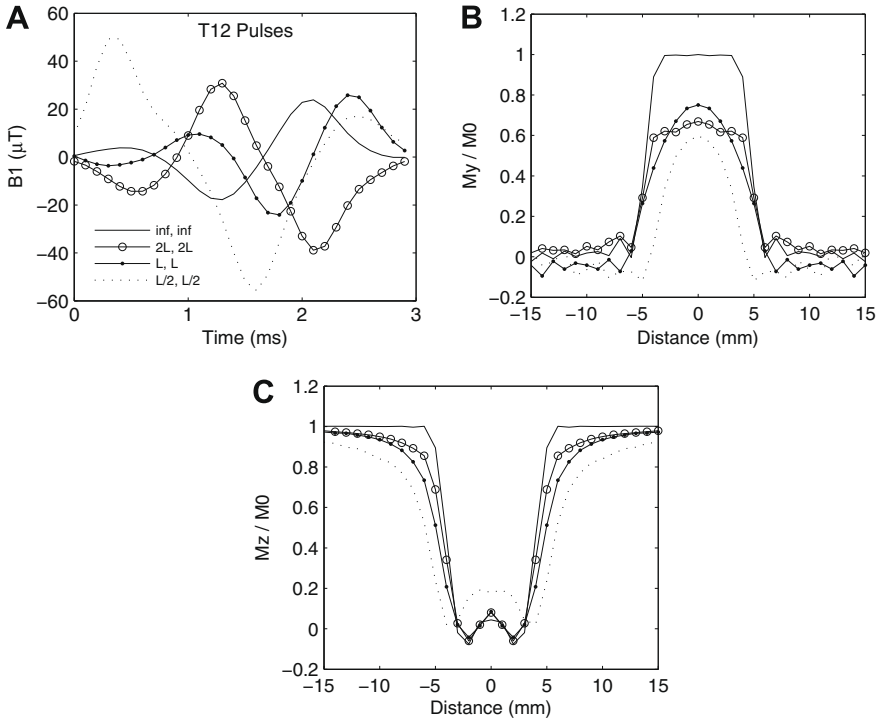

Fig. 5. RF pulses (A) exhibit more excursions than BURPx when optimized under short T1 and T2 simultaneously. The peak power increases with shortening relaxation times. Significant distortion still exists in the absorption profiles due to short T1. Magnetization components appearing in (B–C) do not show monotonic behavior with either T1 or T2 values (i.e. maximum M_y due to T1 = T2 = 2L appears intermediate to the other two M_y profiles) because of the competing effect of the two relaxation times.

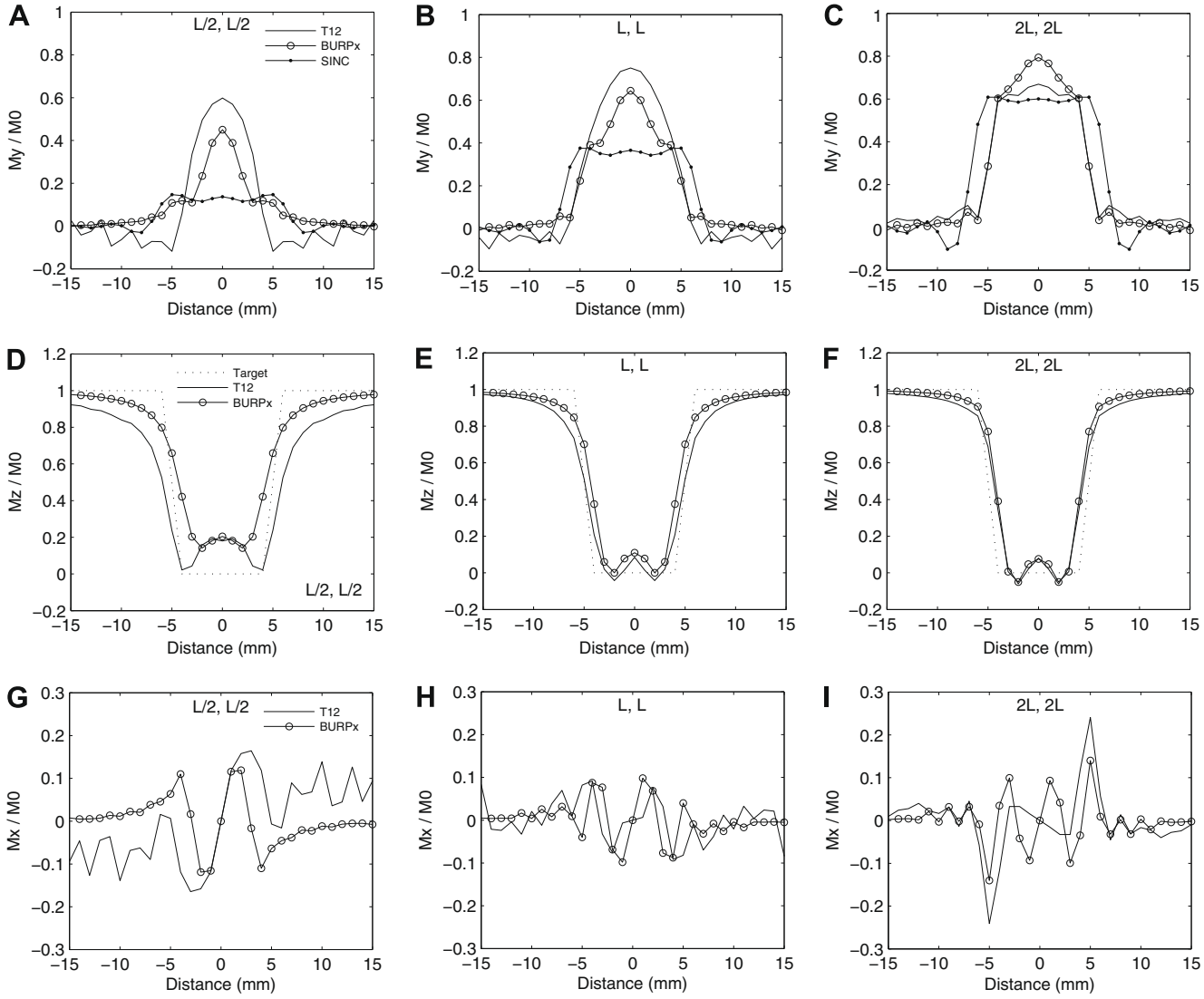

Fig. 6. Comparison between T12 pulses (i.e. optimized under short T1 and T2) with BURPx (i.e. optimized under infinite T1 and T2) and standard sinc pulses. Magnetization is calculated under short T1 and T2 as shown in the title of the figures. Absorption magnetization is larger for the T12 pulses (under T1 = T2 = $L/2$ and L only) with significant distortion due to short T1. The penalty is more oscillations and slightly larger peaks in the undesired dispersion profiles (G–I). The longitudinal profiles are similar (D–F).

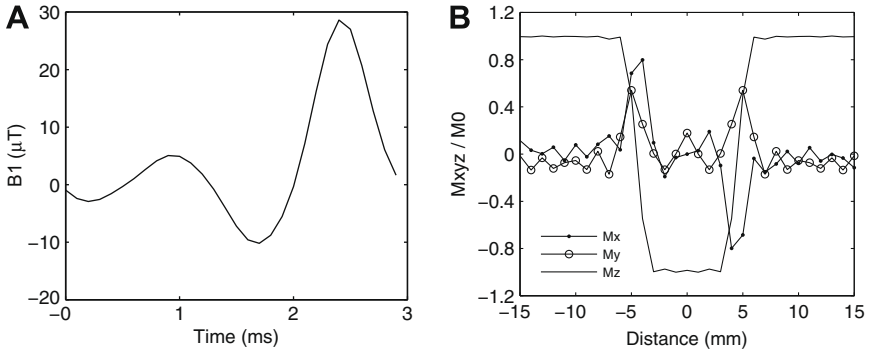

Fig. 7. Self-refocused π inversion pulse optimized under both T1 = T2 $\sim$ inf (A). This is basically the standard pulse produced by Geen and Freeman [1]. Although inverted magnetization has good shape the remaining transverse magnetization is large (B).

T1 $\sim$ inf, and T2 = L) to samples with different values of T1 and T2. In particular we show that magnetization profiles are stable (e.g. M_y never exceeds M_0) even when T1 is short (i.e. faster magnetization recovery) or when T2 is long (i.e. slower magnetization decay) as shown in Fig. 9. For many of the pulses developed in this work we have listed the Fourier coefficients of the RF pulses in Table 1.

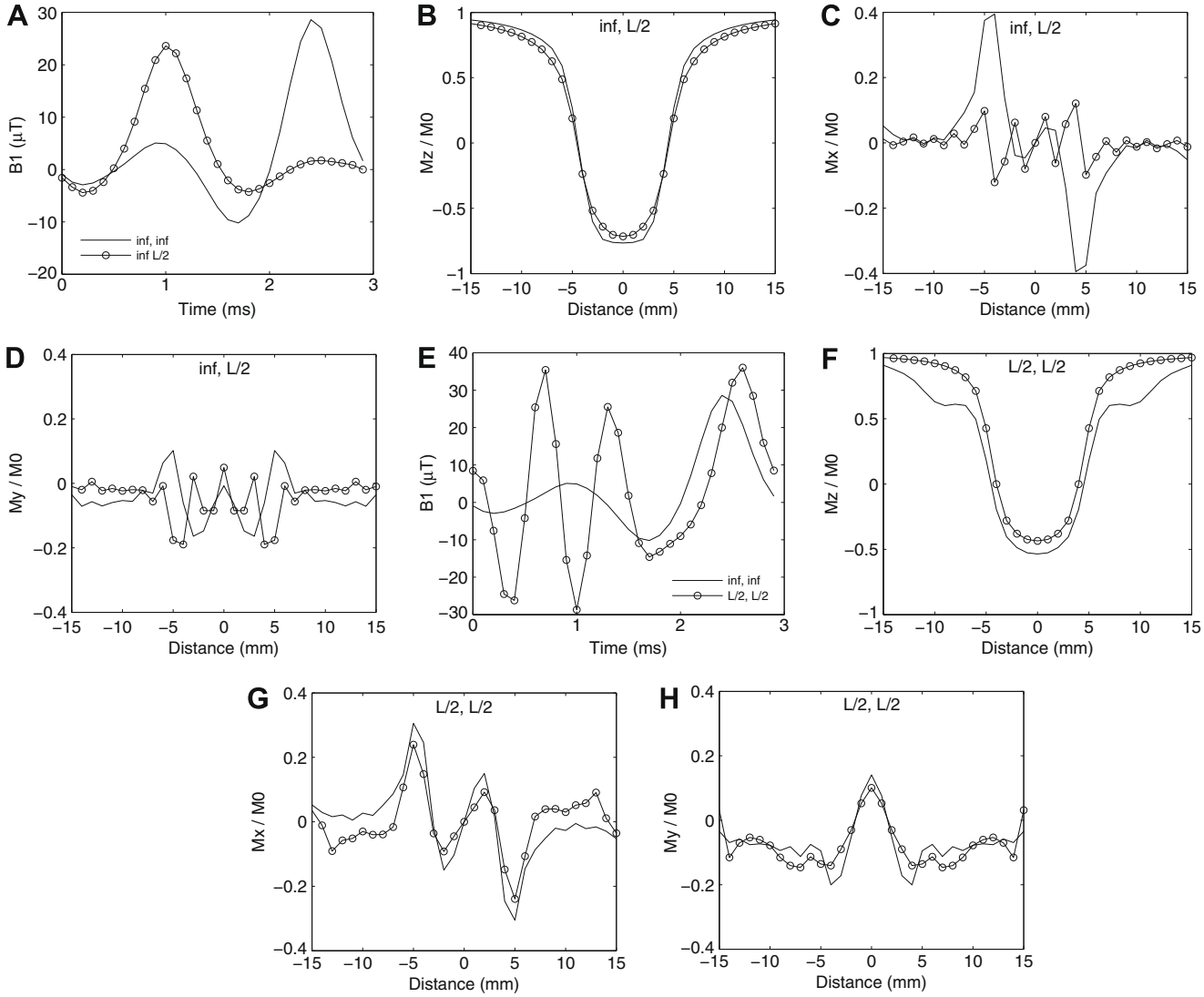

Fig. 8. New self-refocused π inversion pulses optimized under various values of T1 and T2 simultaneously. The new pulses are compared with the standard pulse (A). (A–D) shows the effect of the new pulse in suppressing remaining dispersion component when T2 alone is reduced to $L/2$. When both T1 and T2 are reduced to $L/2$ (E–H) the new pulse manages to improve the severely distorted inverted magnetization on the expense of a more complex RF profile. No further suppression of transverse magnetization is achieved.

4. Discussion and conclusions

Many studies have concentrated on the analysis of magnetization behavior under conditions of short relaxation times compared to RF pulse duration [2–6]. This is usually accomplished by inserting the relaxation terms into the Bloch differential equations and forward calculating magnetization solution using numerical simulations. Changing the value of T2 while assuming an infinite value of T1, or changing both T1 and T2 simultaneously elucidates the effects of relaxation on the transverse and longitudinal magnetization components. In this work, we have studied self-refocused RF pulses where gradient reversal is eliminated from the slice selection process. Our results confirm those obtained previously by other workers [3,5] that short T2 values severely attenuate transverse magnetization while the longitudinal component is unaffected. Short T1 (which is accompanied by short T2 due to the limitation $T2 \leqslant T1$) leads to additional distortion of the absorption profile and broadening of the longitudinal profile.

Other studies have attempted to design RF pulses that combat the effects of short relaxation times [7–9,16–20]. These were preceded by the original work of Torrey [21] in which a rectangular RF pulse was applied and an analytical solution to Bloch equations was sought. In order to find an analytical solution most of the above workers had to make certain assumptions about many factors such as resonance conditions, small tip angle excitation, etc. Nuzzilard and Freeman [7] adopted a similar approach to ours by effectively attenuating the target profile by a numerical factor based on relaxation times. An average value was chosen to account for both small relaxation losses when the magnetization vector lies near the z-axis, and large relaxation losses when the vector is near the transverse plane. No RF profiles were reported in their work but only magnetization responses. Our approach continuously calculates the magnetization reduction factor instantaneously at all stages of the magnetization vector rotation under the effect of the RF pulse.

This approach yielded more T2-relaxation efficient RF pulses. For a $\pi/2$-excitation the pulse (SDETR) produced under the condition $T2 = L/2$ contains a single large peak delayed to the end of pulse

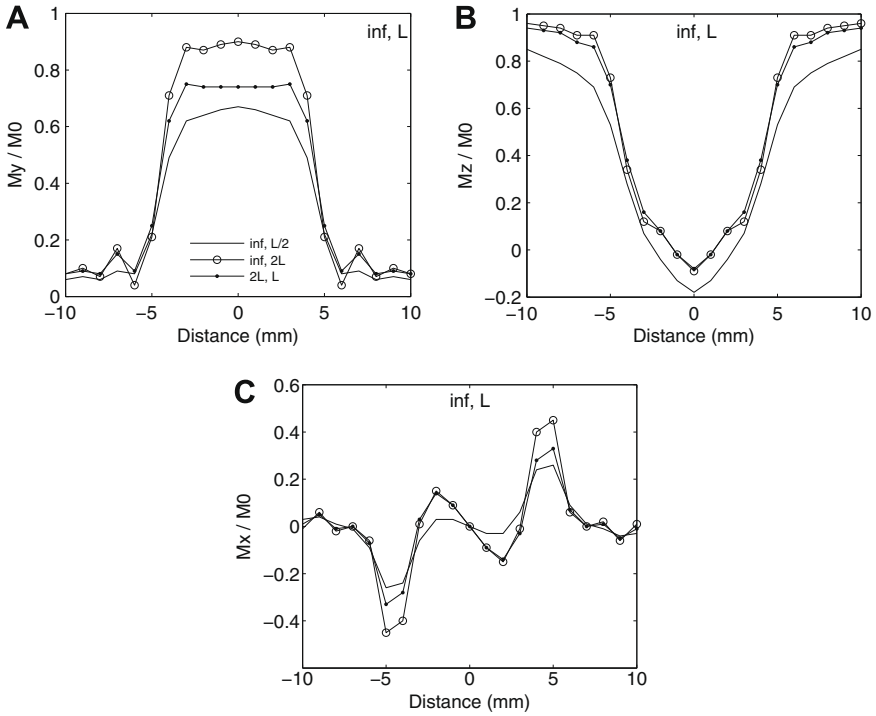

Fig. 9. The magnetization response calculated for different values of T1 and T2 (as shown in the legend). However, the RF pulse used was optimized under T1 $\sim$ inf and T2 = *L*. The bounded magnetization emphasizes the stability of these pulses and their usefulness because their application is not limited to the value it was optimized for only.

Table 1
Fourier coefficients (in μT) for various pulses used in this work. The values of relaxation times are given and also the figure number where the pulse appeared.

Pulse type	BURP	BURPx	BURPx	SDETR	T12	T12	T12	T12
Flip	90	90	90	90	90	180	180	180
T1	Inf	Inf	Inf	Inf	*L*/2	Inf	Inf	*L*/2
T2	Inf	Inf	2*L*	$\leqslant L$	*L*/2	Inf	*L*/2	*L*/2
Figure	1D	1D	3A	3A	5A	7A	8A	8I
a_0	2.244	1.885	2.000	−5.792	1.956	3.688	3.498	3.696
a_1	8.299	5.601	9.036	−4.387	29.612	6.290	−5.264	7.045
a_2	−11.031	−9.997	−9.051	3.594	−15.819	−4.268	−0.209	3.765
a_3	0.809	2.316	−3.681	2.983	−5.458	−3.649	2.081	−5.078
a_4	0.441	0.455	0.960	0.712	−4.404	−0.921	−0.687	10.723
a_5	0.289	−0.286	0.712	−0.274	−1.384	0.169	0.421	−7.036
a_6	−0.273	−0.122	0.651	−0.307	1.204	0.342	0.161	−4.614
b_1	−7.884	−8.918	−4.101	8.262	17.644	−4.994	5.638	−2.676
b_2	0.151	4.728	−11.749	6.879	−3.805	−10.590	−8.268	−12.661
b_3	2.140	1.020	5.177	0.043	6.307	0.543	1.797	−9.686
b_4	0.397	−0.215	1.412	−0.925	−4.338	1.192	0.001	−0.552
b_5	−0.462	−0.435	0.538	−0.400	−0.837	0.656	−0.319	11.909
b_6	−0.072	0.240	−0.431	0.037	−1.510	0.047	0.195	−2.347

duration. This ensures that little magnetization exists near the transverse plane subject to T2 relaxation. Significantly, the peak amplitude of this new pulse is only 23% greater than that optimized under infinite T2 while its energy (the sum of the amplitude squared) is less by 9%. This is characteristically similar to minimum energy pulses profiles found analytically by inverse scattering transform [22]. A similar pulse was optimized for inversion with good performance under short T2 values. In this case a smaller amplitude excursion (Fig. 8A) is needed to fully invert magnetization while at the same time reducing the transverse magnetization significantly (Fig. 8C). This is very important since it would not be useful (time wise) if one has to apply dephasing lobes after a RF pulse which is meant to be a self-refocused pulse. When both T1 and T2 are shorter than the pulse duration the optimized pulse managed to improve the inverted profile significantly (Fig. 8F), however, on the expense of fast varying B1 profile associated with large energy (Fig. 8E).

The bounded magnetization values (shown in Fig. 9) emphasize the stability of these pulses and their usefulness because their application is not only limited to the relaxation times they were optimized for.

Although some RF profiles have been presented here, many (indeed infinite [1,9,22]) solutions exist when searching for a global minimum in a large dimensional space. The choice of search parameters can lead to many different RF solutions with similar magnetization profiles. For example, we have found that increasing the maximum number of search steps (e.g. from $N = 3000$ to $N = 30{,}000$) may produce similar overall error values, however, with no unique RF solution. Some of these profiles are undesirable because they may have many excursions or large peak values. Also, changing the weighting factors (α_i) can force the solution to switch between BURPx and SDETR profiles under short T2 conditions. In dimensionally large optimization problems, single error value is

Table 2
The search procedure converges to different RF solutions according to the values of various parameters used in the optimization algorithm. T_0 is the initial annealing temperature, ΔT is the temperature step, ε_{Obj} is the tolerance for the overall objective function while ε_{lower} and ε_{upper} are the lower and upper tolerance values for the magnetization amplitudes. α_i are the weighting factors associated with the objective function.

Profile	1	2	3	4
# Fourier Coef.	6	6	6	6
w ($\times w_0$)	1.0	1.0	1.0	1.0
ε_{lower} and ε_{upper}	0.001	0.001	0.001	0.01–0.1
ε_{Obj}	0.0001	0.0001	0.001–0.01	0.0001
N	10,000	3000–10,000	10,000	10,000
T_0	2.0	2.0	2.0	2.0
ΔT	0.1	0.005–0.1	0.1	0.1
α_i	0.1–4.0	0.1–4.0	0.1	0.1
T1	Inf	Inf	Inf	Inf
T2	Inf	L	L	L

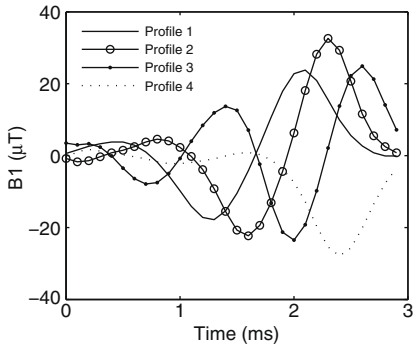

Fig. 10. Some RF profiles produced by different choices of the optimization parameters as listed in Table 2.

not usually sufficient to decide on the optimum profile. One has to also consider the shape of the profile produced and in particular the number of excursions and maximum peak amplitudes. We have summarized few parameter values among the many we have investigated in Table 2 along with few RF profiles produced (Fig. 10). For example, an increase in the number of Fourier coefficients may limit the effect of other parameters such as the number of iterations or renders the solution unstable. We are considering further quantification of the effects of the optimization parameters for future work.

Acknowledgment

This work was financially supported by the Research Affairs at the UAE University under a contract No. 02-02-2-11/04.

References

[1] H. Geen, R. Freeman, Band-selective radiofrequency pulses, J. Magn. Reson. 93 (1991) 93–141.
[2] T.J. Lawry, G.S. Karczmar, M.W. Weiner, G.B. Matson, Computer simulation of MRS localization techniques: an analysis of ISIS, Magn. Reson. Med. 9 (1989) 299–314.
[3] A. Raddi, U. Klose, Relaxation effects on transverse magnetization using RF pulses long compared to T2, J. Magn. Reson. 144 (2000) 108–114.
[4] J.D. Pearlman, T.J. Wieczorek, Relaxivity corrected response modulated excitation (RME): a T2-corrected technique achieving specified magnetization patterns from an RF pulse and a time varying magnetic field, Magn. Reson. Med. 32 (1994) 388–395.
[5] P.J. Hajduk, D.A. Horita, L.A. Lerner, Theoretical analysis of relaxation during shaped pulses. I. The effects of short T1 and T2, J. Magn. Reson. A 103 (1993) 40–52.
[6] W.S. Warren, S.L. Hammes, J.L. Bates, Dynamics of radiation damping in nuclear magnetic resonance, J. Chem. Phys. 91 (1989) 5895.
[7] J.-M. Nuzillard, R. Freeman, Band-selective pulses designed to accommodate relaxation, J. Magn. Reson. A 107 (1994) 113–118.
[8] K. Zangger, M. Oberer, H. Sterk, Pure-phase selective excitation in fast-relaxing systems, J. Magn. Reson. 152 (2001) 48–56.
[9] E. Kupce, J. Boyd, I.D. Campbell, Short selective pulses for biochemical applications, J. Magn. Reson. B 106 (1995) 300–303.
[10] S. Kirkpatrick, C.D. Gellat Jr., M.P. Vicchi, Optimization by simulated annealing, Science 220 (1983) 671–680.
[11] C.J. Hardy, P.A. Bottomly, M. O'Donnell, P. Roemer, Optimization of two-dimensional spatially selective NMR pulses by simulated annealing, J. Magn. Reson. 77 (1988) 233–250.
[12] W.H. Press, S.A. Teukolsky, W.T. Vetterling, B.P. Flannery, Numerical Recipes in Fortran: The Art of Scientific Computing, second ed., Cambridge University Press, Cambridge, 1992.
[13] R.J. Schilling, S.L. Harris, Applied Numerical Methods Using MATLAB and C, Brooks/Cole, 1999.
[14] S.S. Rao, Optimization Theory and Applications, Wiley, New Delhi, 1987.
[15] E. Lunati, P. Cofrancesco, M. Villa, P. Marzola, F. Osculati, Evolution strategy optimization for selective pulses in NMR, J. Magn. Reson. 134 (1998) 223–235.
[16] F. Schick, Excitation of narrow frequency bands with reduced relaxation-related signal losses: methodology and preliminary applications, Magn. Reson. Imag. 17 (1999) 527–536.
[17] C. Roumestand, D. Canet, N. Mahieu, F. Toma, DANTE-Z, an alternative to low-power soft pulses. Improvement of the selection scheme and applications to multidimensional NMR studies of proteins, J. Magn. Reson. A 106 (1994) 168–181.
[18] D. Boudot, D. Canet, J. Brondeau, J.C. Boubel, DANTE-Z. A new approach for accurate frequency selectivity using hard pulses, J. Magn. Reson. 83 (1989) 428–439.
[19] G.A. Morris, P.B. Chilvers, General analytical solutions of the Bloch equations, J. Magn. Reson. A 107 (1994) 236–238.
[20] N. Khaneja, T. Reiss, B. Luy, S.J. Glaser, Optimal control of spin dynamics in the presence of relaxation, J. Magn. Reson. 162 (2003) 311–319.
[21] H.C. Torrey, Transient nutation in nuclear magnetic resonance, Phys. Rev. 76 (1949) 1059–1068.
[22] J. Magland, C.L. Epstein, Exact half pulse synthesis via the inverse scattering transform, J. Magn. Reson. 171 (2004) 305–313.